Flash joining of conductive ceramics in a few seconds by flash spark plasma sintering

Mattia Biesuz [a,b,#], Theo G. Saunders [a], Salvatore Grasso [c], Giorgio Speranza [d], Gian D. Sorarù [b], Renzo Campostrini [b], Vincenzo M. Sglavo [b], Michael J. Reece [a]

[a] Queen Mary University of London, School of Engineering and Materials Science

[b] University of Trento, Department of Industrial Engineering, Via Sommarive 9, 38123, Trento, Italy

[c] Key Laboratory of Advanced technologies of Materials, Ministry of Education, School of Materials Science and Engineering, Southwest Jiaotong University, Chengdu 610031, China

[d] CMM - FBK, Via Sommarive 18, 38123 Trento, Italy

[#] Corresponding author: M.B. mattia.biesuz@outlook.com

Abstract

The feasibility of conductive ceramics flash joining using spark plasma sintering is demonstrated. It is shown that graphite disks can be joined in a few seconds (6 – 10 s electric discharge time) using a SiOC precursor (methyl silicone resin) as an interlayer. Differently from usual flash experiments, the process does not require any pre-heating, allowing a dramatic reduction of the processing time. XPS analysis of the joint revealed a clear evolution of the chemical environment of silicon with a progressive transition from SiOC to SiO_2/SiC. Mechanical tests were performed to determine the fracture toughness (1.0 ±0.2 MPa $m^{0.5}$) and fracture energy (40.6 ± 9.8 J/m^2) of the interface.

Flash joining can be applied beyond graphite joining, and opens a novel and flexible processing route for many conductive ceramics, as demonstrate by preliminary work on Kanthal® Super $MoSi_2$ and C_f-reinforced SiC.

1 Introduction

Ceramics are characterized by poor machinability and high melting temperature. Therefore, it is often difficult to manufacture them as net-shape components with large and complex geometry. To overcome this, different joining technologies have been developed to produce strong and temperature resistant ceramic-ceramic and ceramic-metal joints, among them: diffusion bonding [1]; nanocrystalline interlayer joining [2,3]; transient eutectic-phase joining [4]; MAX-phase joining [5]; transient liquid phase joining (where the liquids are glasses and glass ceramics [6], oxynitrides [7] or metals [8]). In addition, joints can be produced by applying pre-ceramic polymers between two ceramic components [9–11]. The pre-ceramic polymer is cross-linked and heat treated in a protective atmosphere to produce a ceramic interlayer (SiOC, SiO_2, SiC, Si_3N_4 and others depending on the resin composition [10]). However, such a joining process is very slow as very low heating rates (i.e.,1°C/min [11]) are generally employed to allow the gases evolved during the polymer-to-ceramic transition to be removed.

In recent years, flash sintering (FS) has emerged as a promising current-assisted sintering technology for ceramics, where the internal generation of heat by the Joule effect [12] allows rapid particle welding and consolidation [13–15]. The mechanisms of flash sintering are not yet fully understood [16–24]. Extremely rapid diffusion is one of the signatures of flash sintering, which paves the way to novel processes besides just sintering, among them: synthesis [25–29]; field-induced glass softening [30–32]; plastic shaping [33]; microstructural modifications [34]; and joining. Flash joining (FJ) processes are currently being developed. These, are mainly focused on the production of ceramic-metal joints, such as: C_f - SiC composites to Ti [35] or Ti-Nb-Ti interlayers [36]; and YSZ to Ti [37] or Ni alloys [38]. Recently, Xia et al. also produced the first ceramic-ceramic joint in YSZ using a flash process [39].

Graphite and carbon-based materials are of great technological interest because of their exceptional heat resistance and electro/thermal properties, with applications ranging from the aerospace to nuclear industries [40–42]. Graphite is usually bonded using interlayers constituted by metals able to form carbides [40–42], which ensures mechanical adhesion of graphite to the metal itself. Other, conductive ceramics are also of increasing interest to the ceramic community, like borides, silicides, MAX-phases and others.

In this work, we demonstrate the feasibility of flash joining of electrically-conductive ceramics using a spark plasma sintering machine. The focus is on graphite components joined using a polymer-derived ceramic (PDC) interlayer. The proposed process allows ultra-fast joining of such a refractory material, without the limitations imposed by using the more common metallic interlayers (i.e., metals often lose their mechanical properties at high temperature and have poor resistance to oxidation/corrosion compared with ceramics). In order to show the flexibility of the process, preliminary results on Kanthal® Super $MoSi_2$ and C_f-reinforced SiC are also reported.

2 Experimental procedures

Graphite disks of Durograph 20 grade of 3 mm thick and 20 mm in diameter were used in this work (density = 1.84 g/cm^3; open porosity = 10%; electrical resistivity 14 μΩ m). The same graphite grade was used for the FSPS tooling. The adjoining surfaces were mechanically polished using a 3 μm diamond paste. Some joining experiments were also carried out on C_f-reinforced SiC (SigraSiC) purchased from Erodex Ltd (UK). The adjoining surfaces were polished down to 800 grit diamond paper. The SigraSiC samples were 20 mm diameter and 5 mm thickness. The pre-ceramic polymer used as the interlayer was a methyl silicon resin (Silres MK, Wacker, Germany). 5 g of the solid resin was dissolved in 6 g of acetone; 4 drops of solution was used as an interlayer between the two facing graphite surfaces. The 5:6 resin-to-acetone ratio was chosen because it allowed a complete dissolution of the polymer and the obtained solution had a relatively low viscosity (easy to manipulate with a pipette). This ratio might be anyway object of future optimizations. An external load of 3 kg was applied while drying the solution in air for 20 min.

The obtained components were then subjected to flash-spark plasma sintering (F-SPS) using a SPS system HPD 25/1, FCT systems (Germany). The samples were introduced between to graphite punches (diameter of 20 mm) and subjected to an external load of 40 MPa. The system composed of the sample

and the graphite punches was thermally insulated by wrapping them with a graphite felt. During F-SPS the SPS was operated at full power, which corresponded to about 9 V electrical potential. While 9 V was provided by the transformer, in the SPS about 2.5 V was lost to the internal diode. The gave a usable electrical potential of 6-7 V. Different treatment times were employed from between 6 and 10 s. The temperature during the process was checked at 4 mm from the sample using the SPS top pyrometer pointed at the hole in graphite punch.

For comparison, a conventionally joined graphite sample was also prepared. In this case the sample was pyrolised at 1200°C under pressureless conditions in an Ar atmosphere. The heating rate was 3°C/min, the soaking time at high temperature was 30 min and the cooling rate was fixed at 10°C/min down to 500°C (followed by free cooling). The process was carried out in a Lenton tubular furnace. Additionally, to investigate the effect of heating rate, a sample was processed inside the SPS system using a relatively low heating rate and 40 MPa of compressive stress (heating and cooling rate = 10°C/min, T max = 1200°C, dwelling time = 5 min).

Kanthal® Super $MoSi_2$ samples were obtained by cutting 22 mm long cylinders form a heating element for a Nabertherm box furnace. The adjoining surfaces were polished down to 800 grit diamond paper. The diameter of the samples was about 12 mm. The SPS process was carried out limiting the power of the machine to 60 or 70% of the maximum output and applying a clamping pressure of about 50 MPa. The joining time was fixed at 18 s. Shorter treatments at higher power densities were not possible because the samples broke as a result of the thermal shock. Experiments both with and without the methyl silicon resin interlayer were carried out.

All of the obtained samples were cut and polished with SiC papers (down to 4000 grit) and diamond pastes (down to 1 μm grain size). The polished cross section was analyzed by SEM/EDS using a FEI Inspect-F instrument. In order to check the integrity of the carbon fibers of the SigraSiC composite, additional micrographs were taken of its fracture surface. The fracture surfaces were produced as follows: first the material was delaminated using a manual mechanical vice (configuration reported in Supplementary Material, Figure S2), then it was clamp inside a pliers and bent to produce a fracture orthogonal to the lamination plane.

Thermo gravimetric (TG) analysis of the pre-ceramic resin was carried out using a Netzsch STA 409 instrument (Netzsch-Gerätebau GmbH, Germany) by loading about 150 mg of the solid resin into an alumina crucible. Before the test, air was removed three times from the furnace chamber by using a vacuum pump, then the chamber was filled with Ar (purity 99.9999%). The heating rate was 10°C/min. In order to check the ceramization of the resin during the F-SPS process some methyl silicon powder was pyrolised in the SPS system following the same thermal cycle used for joining. To do this, the same set-up used for flash joining was reproduced. However, a hole (8 mm in diameter) was drilled in the center of one of one the graphite disks and some powder was poured in. The pyrolised material was then studied using thermal gravimetric analysis coupled with mass spectrometry, TG-MS (Supplementary material).

Some graphite joints were purposely broken after joining by propagating an interfacial crack, and the joint region was then characterized using XPS. Spectra were collected using an Axis DLD Ultra instrument (Kratos, Manchester UK). To increase the surface sensitivity, spectra were acquired under tilted conditions with an angle of 15°between the sample surface and the analyzer axes.

The graphite samples treated for 6, 8 and 10 s were subjected to mechanical characterization. The samples were cut using a low velocity diamond saw with a thin blade (300 μm) along directions orthogonal to the interface to produce small bars with size of about 3 mm x 20 mm x 6 mm (the latter being the thickness of the original joined disks). The lateral surface of the samples was carefully polished using SiC papers and diamond pastes down to 3 μm. Some of the samples were subjected to indentation tests; Vickers indentations were produced at the interface, taking care to align one of the indenter diagonals with the interface itself. Maximum loads of 29.8 N, 49 N and 98 N were used. The test produced cracks along the interface, whose length was measured using an optical microscope. At least four sets of indentation cracks were measured for each load and processing condition. The interface fracture toughness was evaluated as [43]:

$$K_C^i = \chi \frac{P}{c^{1.5}} \quad (1)$$

where P is the indentation maximum load, c the half-crack length and

$$\chi = 0.016 \left(\frac{E}{H}\right)^{0.5} \quad (2)$$

E and H being the elastic modulus and the hardness of the graphite used in the present work. E was measured using three-point bending tests (span = 16 mm) on small graphite samples (around 3 mm x 3 mm x 18 mm); H was measured using loads of 98 N. It is important to point out here that the interface fracture toughness was evaluated instead of the more rigorous interface fracture energy (G_C^i) [43] because of the very limited thickness of the interface layer.

The other samples cut from the original joined disks were subjected to bending tests for the measurement of the fracture energy according to the procedure proposed by Charalambides et al. [44]. Initially, a thin notch (about 2 mm deep) was produced orthogonally to the interface in one of the two joined graphite bars; the samples were then subjected to bending to allow the propagation towards the interface where in most cases the crack started propagating along the same. The specimen was then unloaded and reloaded in a four-point bending jig (inner and outer span equal to 4 and 16 mm, respectively) with a cross-head speed of 0.1 mm/min and the load (P*) at which the interface crack started to repropagate was recorded. The fracture energy was evaluated as:

$$G_C^i = \frac{M^2}{2E}\left(\frac{1}{I_b} - \frac{1}{I_c}\right) \quad (3)$$

where M is the bending moment within the inner span associated with P*, I_b and I_c being the moment of inertia of the single/uncracked and composite beam, respectively [44].

One last comment regarding an additional parameter that influences the mechanical resistance of an interface, called the phase angle (ψ). This identifies the mixed mode character of the propagating crack along the interface and depends on the loading procedure. For the indentation method the phase angle is relatively small ($\approx 15°$) which means that the mode I (opening mode) prevails over mode II (sliding mode); conversely, four-point bending tests have $\psi \approx 45°$, in which case the two modes of fracture have similar importance.

3 Results and discussion

3.1 Flash joining of graphite

During the flash joining of graphite, the joint was subjected to an electric current of approximately 2.1 kA (≈ 670 A/cm^2); the dissipated electric power was about 20 kW (Figure 1).

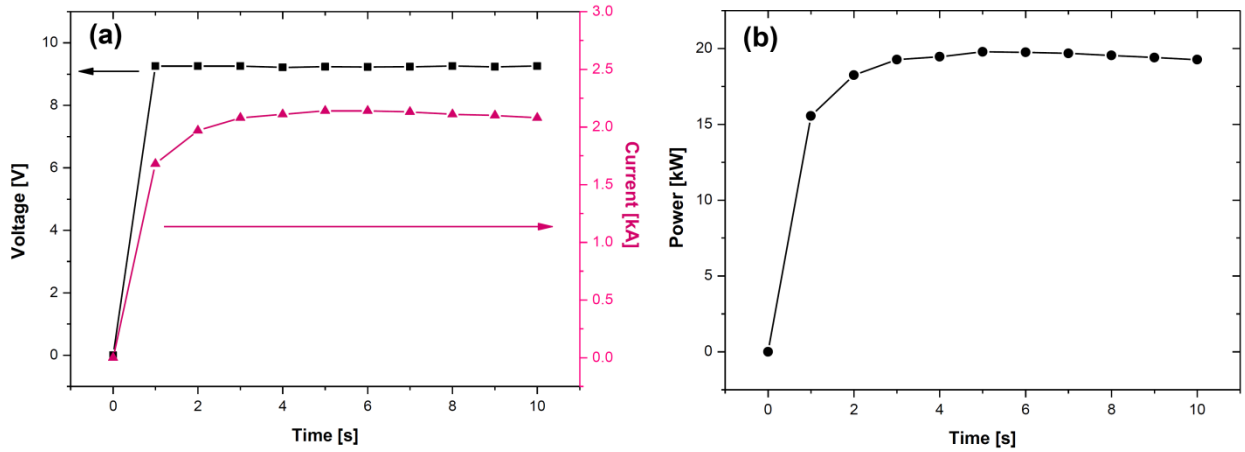

Figure 1: (a) Voltage and current and (b) electric power dissipated during flash joining of graphite.

This caused a rapid, "flash-like", heating of the adjoining components, with heating rates exceeding 155°C/s. This heating rate is about 4 orders of magnitude larger than the rates commonly used for joining ceramics with PDC interlayers [11]. A detailed description of the temperature evolution of the material, as measured by the SPS top pyrometer focused at 4 mm from the sample, is shown in Figure 2(a). One can observe that the temperature peaked after a few seconds, whereas the cooling path was much slower, taking place in some minutes, slowed down by the presence of the graphite felt (thermal insulator). The peak temperature recorded by the SPS machine depended on the treatment time and ranged from 1104-1147°C and 1583-1610°C for the samples treated for 6 and 10 s, respectively (Figure 2(a)).

Figure 2(b) shows the TG plot of the methyl silicone resin. The total weight loss at high temperature was between 11 and 12 wt%. The largest part of which took place below 900°C. Thus, we can state that in all cases the treatments were carried out at temperatures ensuring a complete ceramization of the silicone. To check the effective ceramization of the material, TG-MS analysis were carried out on the methyl silicone resin after that it had been subjected to the same thermal cycle used for FJ (6, 8 and 10 s). No significant weight loss was measured up to 1000°C in those samples(Figure S1, "Supplementary material"). Moreover, the no MS signals associated to the typical species evolving from the methyl silicone resin decomposition were detected (i.e., CO_2, CO, CH_4, SiH_4, methyl silane). Thus, we can state that during the flash process the material was properly pyrilysed.

After FJ at any of the tested conditions, the two graphite disks were bonded together. This result is quite "surprising" considering that the heating rates used were 4 orders of magnitude greater than the conventional ones used for PDC joining. The rapid heating was expected to impact negatively on

the joint integrity since it would not leave enough time for the pyrolysis gas products to be evacuated. This idea had limited the choice of heating rate in previous works. However, our results show for the first time (as a proof of the concept), that effective flash PDC joining is possible in only a few seconds under the effect of an external pressure/current.

Figure 3 shows SEM micrographs of the joint region in a graphite sample treated for 8 s. One can observe that the interlayer is extremely thin and is not clearly identifiable using neither secondary nor backscattered electron detectors. However, the EDS map highlights the formation of a layer containing silicon with a thickness of the order of ≈ 1 µm corresponding to the joining area. Other silicon-rich regions can be identified at several microns from the interface; these can be likely ascribed to pores (present in the graphite disks) filled by the resin. Similar micrographs were obtained for all of the test conditions.

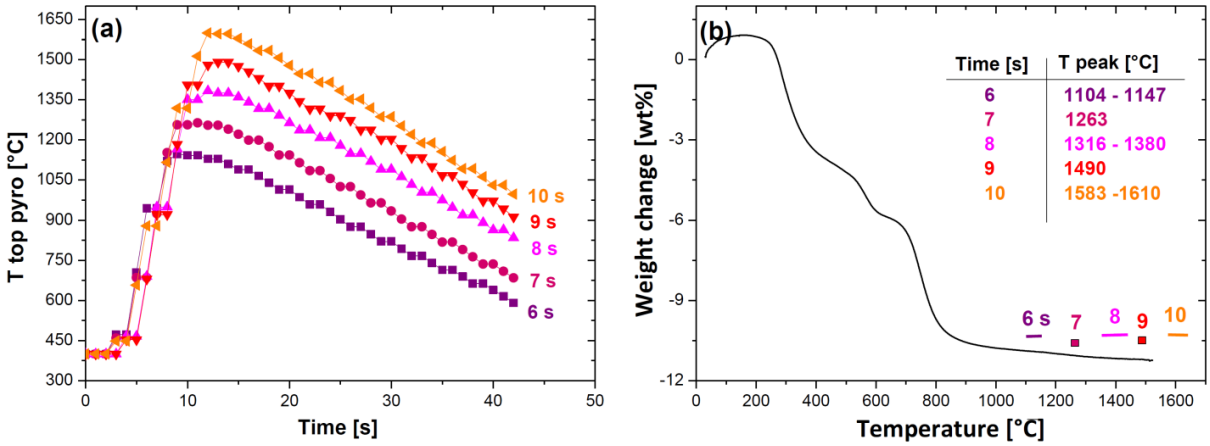

Figure 2: (a) Temperature evolution during FJ of graphite as measured by the top pyrometer of the SPS furnace (pointed at the top punch at 4 mm from the sample), and (b) weight change of the pre-ceramic resin compared with the temperature peak achieved during FJ.

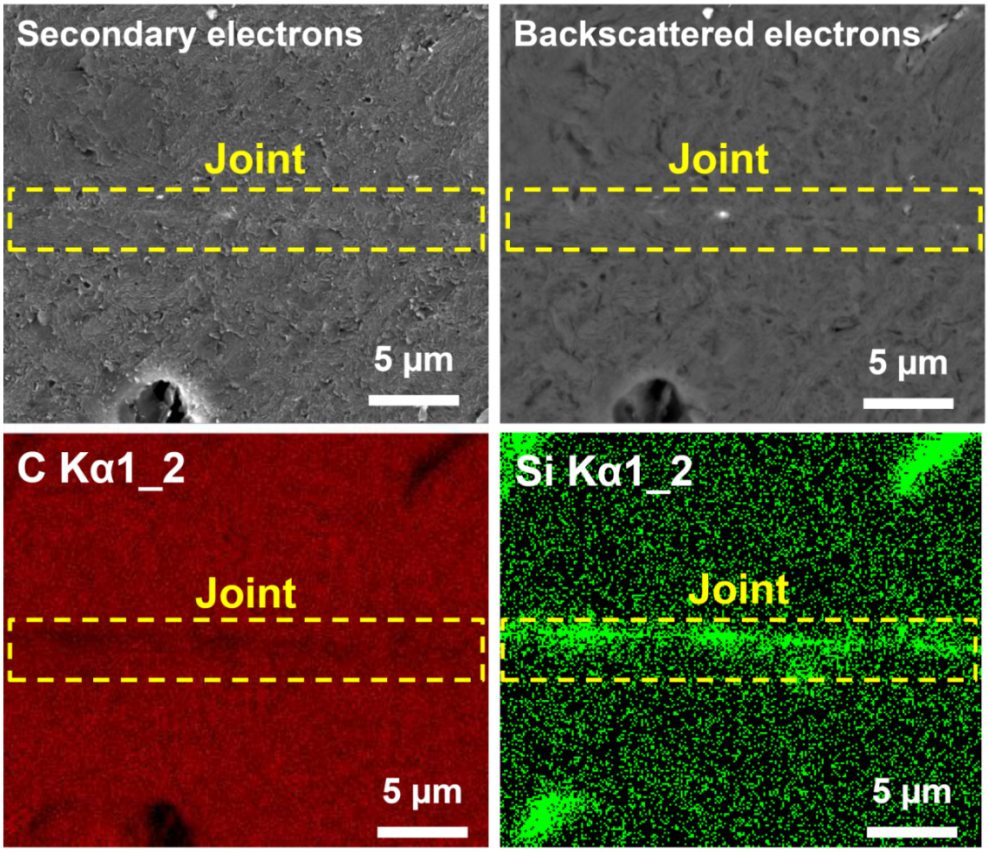

Figure 3: SEM micrographs and EDS mapping of the cross-section of the joint region for a graphite sample FJed in 8 s with PDC interlayer (40 MPa).

It was not possible to obtain satisfactory joints for graphite using a methyl silicone resin interlayer in conventional conditions (pressure-less, 3°C/min up to 1200°C). In this case, a thick (≈ 15 µm) interlayer was obtained showing poor adhesion, large pores, voids and defects (Figure 4(c)). To check whether the microstructural difference could be only ascribed to the application of an external pressure , an additional sample was produced in SPS at a low heating rate (10°C/min up to 1200°C) under a compressive pressure of 40 MPa. Its microstructure appears largely improved compared with the pressure-less sample. However, the interface is slightly more visible than the one produced by FJ (Figure 4 shows a comparison with the sample FJed for 7 s, which reached a similar peak temperature). It seems therefore that the application of high electrical power and extreme heating rates have an effect on the joint microstructure. We can observe that the high heating rate may retard the resin reticulation, thus promoting its deformation. However, this point requires further studies to be confirmed..

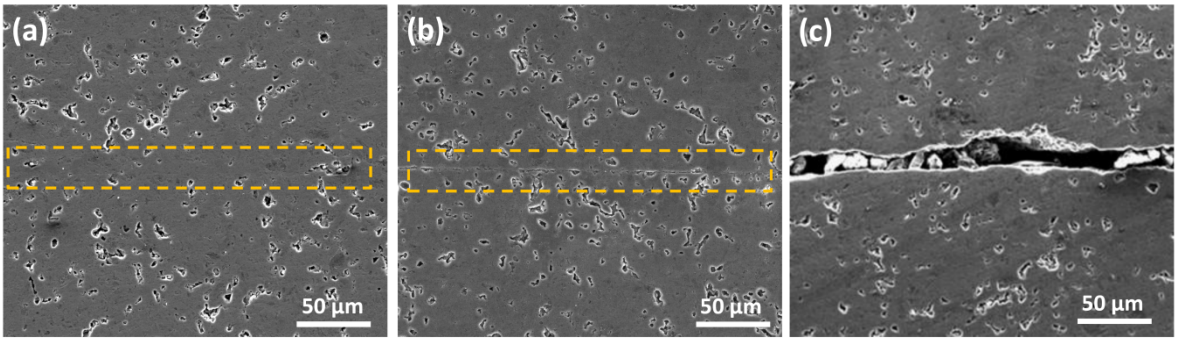

Figure 4: SEM analysis of the polished cross sections of the graphite samples joined with a PDC interlayer: (a) flash joining for 7 s (T peak = 1247°C, 40 MPa); (b) joining inside SPS system at 1200°C and low heating rate (10°C/min); and conventional joining at 1200°C (heating rate = 3°C/min) in flowing argon gas in pressure-less mode. The interface, where not clearly visible, is identified by the dashed-lines.

Considering the thinness of the interlayer, its characterization was carried out using XPS. The XPS Si 2p spectra are shown as a function of the treatment time in Figure 5. One can observe a clear microstructural evolution of the chemical environment of the silicon atoms. The samples treated at the lowest temperatures (treatment times = 6 to 8 s) present a signal consistent with the presence of SiOC, where the silicon is bonded both to O and C. At higher temperature (9 s) a phase separation begins due to a redistribution of the Si-O and Si-C bonds. This leads to the development of a weak shoulder due to the formation of SiC, whereas the SiOC signal shifts to higher binding energies towards the position of SiO_2 (as a result of the lower carbon content in the SiOC). This phenomenon is well-known in SiOC glasses, and usually takes place above 1300-1400°C [45,46]. Therefore, although the treatment time in the current work was very limited, the phase evolution of the system is comparable with that observed under conventional heating. Finally, the sample treated for 10 s presents almost complete phase separation with clear signals due to the presence of SiO_2 and SiC; the latter represents the main chemical environment of silicon. Such a large SiC content cannot be justified considering the initial composition of the pre-ceramic resin, but it suggests that a reaction occurred between the PDC interlayer and the graphite disks. This reveals that the resin interacts with the substrate during the thermal treatment. Indeed, the presence of chemical interactions between the “adhesive” (the PDC) and the substrate (graphite) is a necessary condition to develop adhesion and joining.

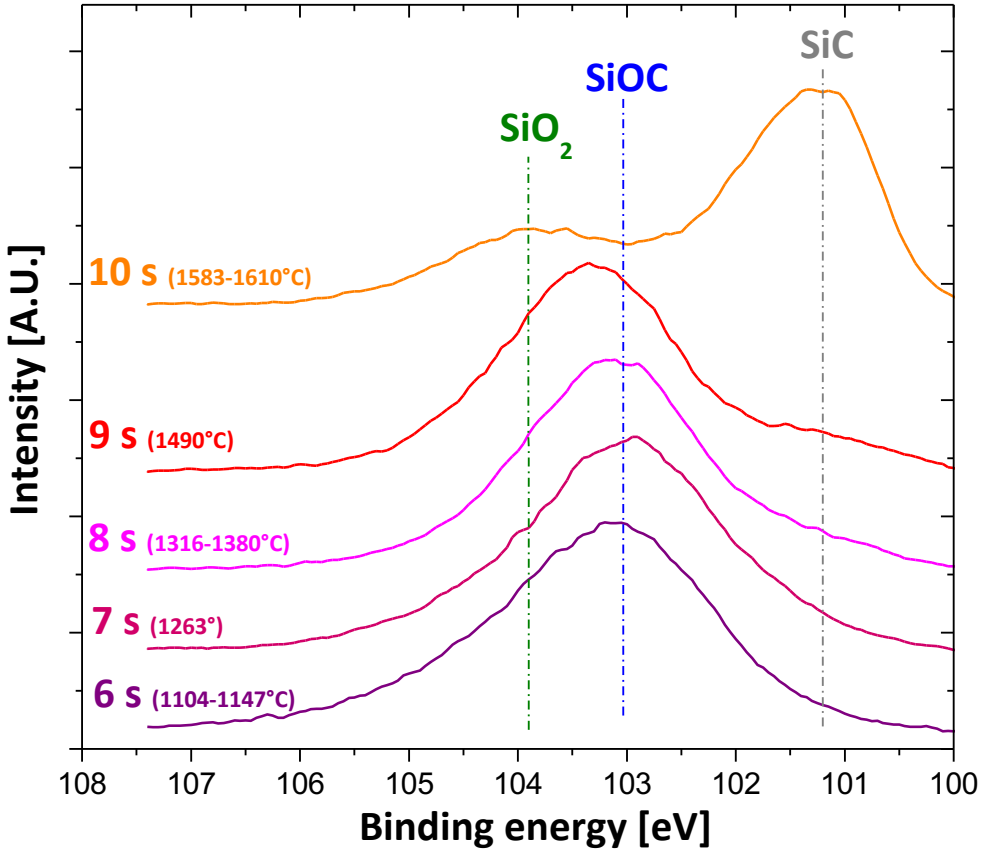

Figure 5: XPS Si 2p spectra of the interface of FJed graphite samples treated for different times with a PDC interlayer.

The results of the mechanical testing on the joint region are reported in Table I. Although the relatively wide scatter in the experimental data, the results are quite interesting. The fracture toughness of the joint is comparable or larger than that typically measured in amorphous materials. It is, moreover, consistent with the values measured on SiOC bulk glasses obtained through the pyrolysis of pre-ceramic polymers [47–49]. This points out that the rapid heating and the thin geometry of the layer do not compromise the material properties. The surface fracture energy, G_C^i, reaches values as high as 40.6 ± 9.8 J/m^2 and surpasses by one order of magnitude the typical values for oxide-based silicate glasses (3.5 – 5.3 J/m^2 [50]). Both fracture toughness and energy increase with the treatment time, revealing that the phase evolution, leading to the formation of SiC (Figure 5), has a positive impact on the joint properties.

Table I : Mechanical properties of the graphite joints with PDC interlayer, processed using 40 Mpa as clamping pressure.

Treating time [s]	K_C^i [Mpa m$^{0.5}$]	G_C^i [J/m^2]
6	0.7 ± 0.3	15.8 ± 7.9

8	0.9 ± 0.2	20.1 ± 4.7
10	1.0 ±0.2	40.6 ± 9.8

It is finally worth mentioning that FJ in the case of conductive ceramics, such as graphite, can be achieved without any pre-heating of the components, which increases the overall processing time during flash sintering of ceramics (it being much slower than the flash discharge itself). Moreover, the reported FJ process has been successfully carried out on relatively large samples (diameter = 20 mm), opening the way to the first possible industrial scale up of a flash-like processes. As a matter of fact, FS is usually carried out on small specimens with cross-section of few mm^2 at the lab scale [16].

3.2 Extension of flash joining to other ceramic conductive systems

In order to prove the flexibility of flash joining in electrically conductive ceramics, we carried out some preliminary experiments on Kanthal® Super $MoSi_2$ and C_f-reinforced SiC. The processing conditions used are reported in Table II.

Kanthal® super finds many applications in the field of high-temperature heating elements. It mainly contains molybdenum disilicide ($MoSi_2$), which is highly electrically conductive (about $2.5x10^6$ S/m at 25°C, $5x10^5$ S/m at 1000°C [51]). $MoSi_2$ possess other properties of technological interest, such as: high melting temperature, good resistance to oxidation, relatively low thermal expansion coefficient and high thermal conductivity [52,53], which enable possible high temperature structural applications [52].

The microstructure of the Kanthal® super flash joined samples is shown in Figure 6. In this case the electrical power was limited to 60 and 70% of the maximum for 18 s; higher power caused damage to the samples due to the thermal shock. The micrographs in Figure 6 reveal that Kanthal® super $MoSi_2$ can be effectively joined in only 18 s by flash SPS. The joint quality appears improved with increasing power output from 60% to 70%. At 70% power the joint is clearly invisible, and the two faying surfaces were firmly welded. Kanthal® super $MoSi_2$ can be effectively joint to itself with or without the use of any PDC (Figure 6). It is known that $MoSi_2$ has a brittle to ductile transition at about 1000°C [52,53], thus we can assume that there was plastic behavior of the material at the FJ conditions. High temperature plastic deformation under the applied stress is likely to be the origin of the joint formation. Although the joining of $MoSi_2$ to metals is well-known [53–56], this work represents to the best of our knowledge the first report of a $MoSi_2$ / $MoSi_2$ joining without the use of metallic interlayers.

We also tested FJ of Cf-reinforced SiC composites, which are attracting increasing interest because of their structural properties [57,58], with important applications in the aerospace industry. In this case, flash joining was carried out using 100% of the maximum power and the external pressure was 40 MPa. The SEM micrographs in Figure 7 reveal that the joint region is highly defective for the lowest treatment time, 6 s, whereas the joint appears well developed with increasing processing times up to 10 s. A thin interlayer originated from the pyrolysis of the pre-ceramic resin can be identified in the latter sample, as shown in the micrographs obtained using the backscattered electron detector in Figure 7. Thus, an effective joint can be obtained in a few seconds without the need of a metallic interlayer, which is commonly used when processing this material [59–62].

In order to verify the integrity of the composite after joining, the microstructure of the FJed samples was compared with that of the as-received composite (Figure 8). No obvious degradation of the carbon fiber was observed as shown in the polished cross-sections presented in Figure 8. However, as a general statement, the composite porosity slightly decreased during FJ because of the high temperature and pressure. Moreover, in all cases the fracture surface of the composite presents clear fiber pull-out and delamination of the fiber-matrix interface. This is key feature of this type of material, providing an effective toughening mechanism. Thus, the microstructural features of the material were substantially maintained after FJ.

Finally, we can mention that the delamination produced by squeezing the samples in a mechanical vice (for sample preparation) followed different path depending on the processing conditions. As a matter of fact, whereas the samples treated for 6 and 8 s broke at the interface between the two joined components, the one treated for 10 s broke elsewhere (Supplementary Material, Figure S3). This suggests that the interface produced by FJ with the PDC interlayer has a mechanical strength comparable with other parts of the component.

Table II: Summary of the treatment conditions used for Kanthal® Super $MoSi_2$ and Cf-reinforced SiC flash joining (current, power and voltage refers to average output of the SPS machine during the joining test).

Sample	PDC interlayer	Limiting power	Treating time [s]	Pressure [MPa]	Current [A/cm^2]	Voltage [V]	Power [kW]	Peak temperature top pyro [°C]*	Joined
Kanthal® Super $MoSi_2$	YES	60%	18	50	900 ± 59	7.30 ± 0.02	7.54 ± 0.23	1150	YES
Kanthal® Super $MoSi_2$	NO	60%	18	50	837 ± 84	7.28 ± 0.03	6.89 ± 0.67	1126	YES
Kanthal® Super $MoSi_2$	YES	70%	18	50	1015 ± 89	7.84 ± 0.02	9.00 ± 0.87	1352	YES
Kanthal® Super $MoSi_2$	NO	70%	18	50	981 ± 116	7.83 ± 0.04	8.69 ± 1.04	1392	YES
C_f- SiC composite	YES	100%	6	40	361 ± 91	9.48 ± 0.06	12.39 ± 2.79	1065	YES
C_f- SiC composite	YES	100%	8	40	395 ± 138	9.53 ± 0.10	11.80 ± 4.03	1281	YES
C_f- SiC composite	YES	100%	10	40	482 ± 145	9.41 ± 0.06	14.22 ± 4.23	1673	YES

** Temperature measured by the top pyrometer of the SPS furnace pointed at 4 mm from the sample on the graphite punch. Since the used materials have an electrical conductivity different form graphite significant deviations are expected in the actual sample temperature.*

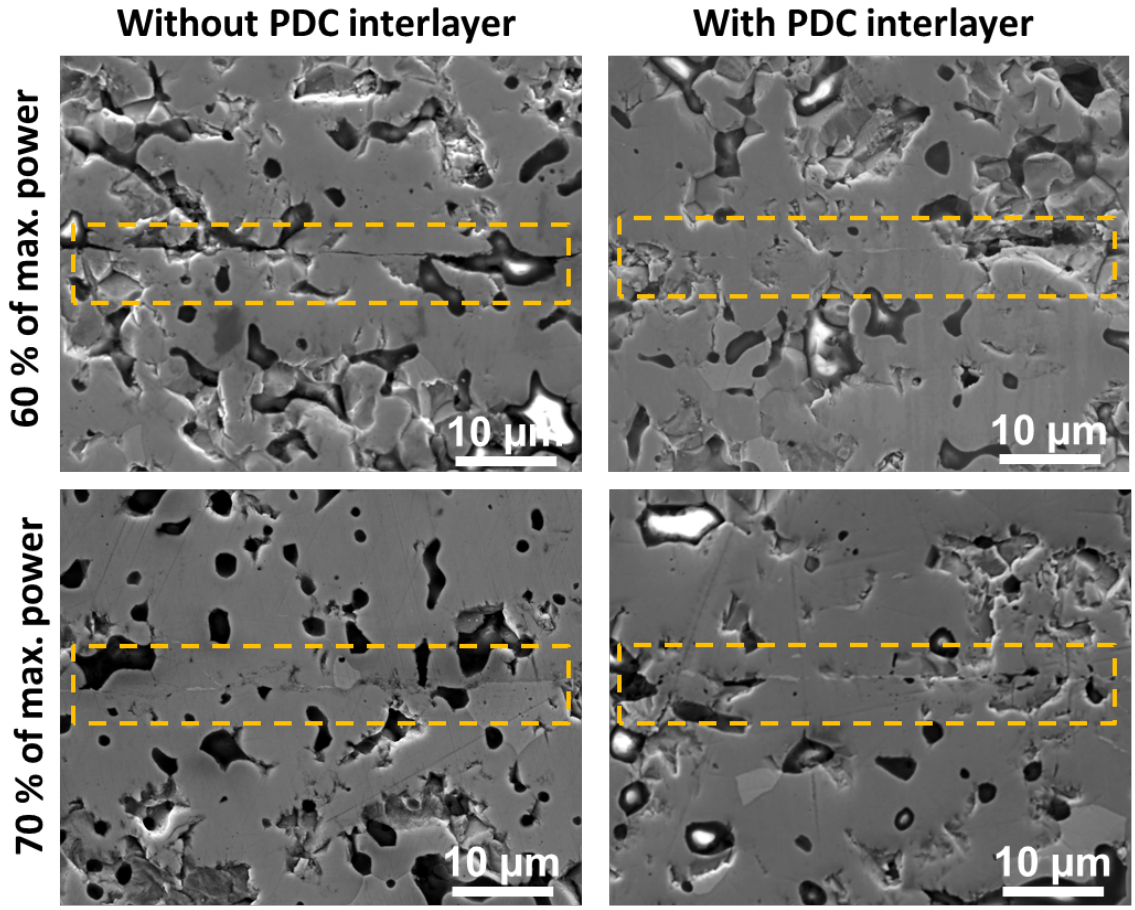

Figure 6: Flash joined Kanthal® Super $MoSi_2$ with and without a PDC interlayer limiting the SPS power to 60% and 70% of the maximum power output for 18 s (50 MPa). Detailed electrical data are available in Table II.

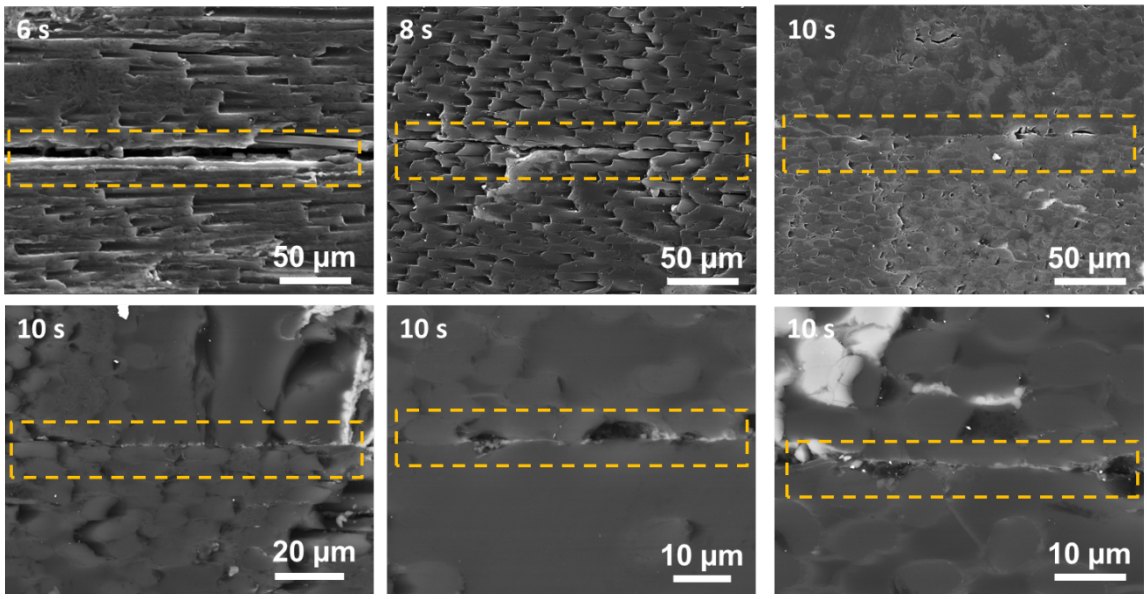

Figure 7: Flash joined C_f – SiC composites with a PDC interlayer using 100% of the SPS relative power and a pressure of 40 MPa. Different microstructures were obtained depending on the joining time: 6, 8 and 10 s (upper line). A thin PDC interlayer is visible in the micrographs taken using the backscattered electrons detector (lower line). Detail electrical data are available in Table II.

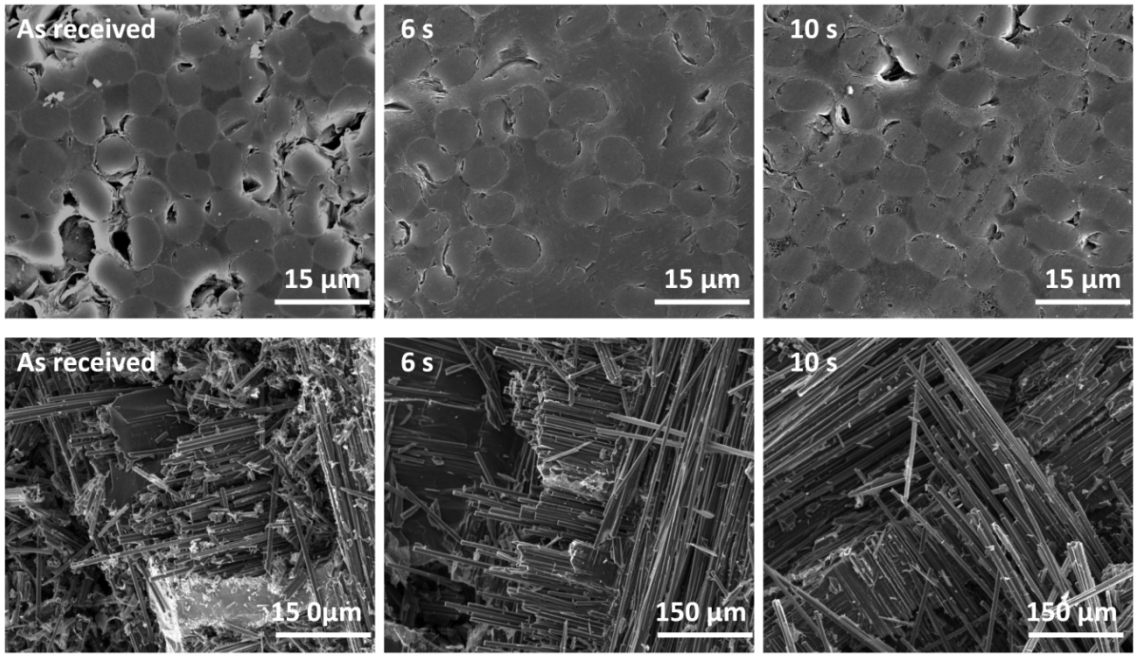

Figure 8: SEM micrographs of C_f – SiC composites before and after flash joining under 40 MPa (detailed electrical data are available in Table II): polished cross-section (upper raw) and fracture surfaces (lower raw).

4 Conclusions

Conductive ceramics can be easily flash joined using SPS in a few seconds, without the need of any pre-heating. The process is highly flexible and applicable to different ceramic systems. As a proof of the concept, in this work we joined graphite (6 – 10 s, ≈ 670 A/cm^2), C_f – reinforce SiC (6 – 10 s, ≈ 360 – 480 A/cm^2) and Kanthal® Super $MoSi_2$ (18 s, ≈ 840 – 1020 A/cm^2). All of the joints had cross sectional areas of the order of a few cm^2, which surpasses by an order of magnitude the ones typically used in flash sintering experiments; thus, this work opens a possible way to the first industrial applications of flash-like processes.

The main focus of the work was on graphite joined with a methyl silicone interlayer (precursor of SiOC). This produced an extremely thin joint. Its structural evolution, investigated by XPS, revealed a progressive transformation of the SiOC interlayer into SiO_2 and SiC, as the processing time (and temperature) increased. The mechanical characterization revealed interfacial fracture toughness and energies as high as 1.0 ±0.2 MPa m$^{0.5}$ and 40.6 ± 9.8 J/m^2, respectively.

Acknowledgements

The authors gratefully acknowledge the JECS Trust for funding the visit of M. Biesuz to the Queen Mary University of London (Contract No. 2018172).

This material is based upon work supported by the Air Force Office of Scientific Research under award number FA9550-17-1-0526.

References

[1] S. Rizzo, S. Grasso, M. Salvo, V. Casalegno, M.J. Reece, M. Ferraris, Joining of C/SiC composites by spark plasma sintering technique, J. Eur. Ceram. Soc. 34 (2014) 903–913. doi:10.1016/j.jeurceramsoc.2013.10.028.

[2] R. Chaim, B.G. Ravi, Joining of alumina ceramics using nanocrystalline tape cast interlayer, J. Mater. Res. 15 (2000) 1724–1728.

[3] B.G. Ravi, R. Chaim, Joining of ZrO 2 -4 .5 wt % Y2O3 (Y-TZP) ceramics using nanocrystalline tape cast interlayers, J. Mater. Sci. 37 (2002) 813–818.

[4] Y. Katoh, L.L. Snead, T. Cheng, C. Shih, W.D. Lewis, T. Koyanagi, T. Hinoki, C.H. Henager, M. Ferraris, Radiation-tolerant joining technologies for silicon carbide ceramics and composites, J. Nucl. Mater. 448 (2014) 497–511. doi:10.1016/j.jnucmat.2013.10.002.

[5] P. Tatarko, V. Casalegno, C. Hu, M. Salvo, M. Ferraris, M.J. Reece, Joining of CVD-SiC coated and uncoated fibre reinforced ceramic matrix composites with pre-sintered Ti3SiC2MAX phase using Spark Plasma Sintering, J. Eur. Ceram. Soc. 36 (2016) 3957–3967. doi:10.1016/j.jeurceramsoc.2016.06.025.

[6] M. Ferraris, M. Salvo, C. Isola, M. Appendino Montorsi, a. Kohyama, Glass-ceramic joining and coating of SiC/SiC for fusion applications, J. Nucl. Mater. 258–263 (1998) 1546–1550. doi:10.1016/S0022-3115(98)00176-7.

[7] S.J. Glass, F.M. Mahoney, B. Quillan, J.P. Pollinger, R.E. Loehman, Refractory oxynitride joints in silicon nitride, Acta Mater. 46 (1998) 2393–2399. doi:10.1016/S1359-6454(98)80021-9.

[8] M. Patel, V. Singh, S. Singh, V. V. Bhanu Prasad, Micro-structural evolution during diffusion bonding of C-SiC/C-SiC composite using Ti interlayer, Mater. Charact. 135 (2018) 71–75. doi:10.1016/j.matchar.2017.11.031.

[9] D.H. Jeong, A. Septiadi, P. Fitriani, D.H. Yoon, Joining of SiCf/SiC using polycarbosilane and polysilazane preceramic mixtures, Ceram. Int. 44 (2018) 10443–10450. doi:10.1016/j.ceramint.2018.03.061.

[10] P. Colombo, G. Mera, R. Riedel, G.D. Sorarù, Polymer-derived ceramics: 40 Years of research and innovation in advanced ceramics, J. Am. Ceram. Soc. 93 (2010) 1805–1837. doi:10.1111/j.1551-2916.2010.03876.x.

[11] P. Colombo, V. Sglavo, E. Pippel, P. Colombo, Joining of reaction-bonded silicon carbide using a preceramic polymer, J. Mater. Sci. 33 (1998) 2405–2412. doi:10.1023/A:1004312109836.

[12] R.I. Todd, E. Zapata-Solvas, R.S. Bonilla, T. Sneddon, P.R. Wilshaw, Electrical characteristics of flash sintering: Thermal runaway of Joule heating, J. Eur. Ceram. Soc. 35 (2015) 1865–1877. doi:10.1016/j.jeurceramsoc.2014.12.022.

[13] M. Cologna, B. Rashkova, R. Raj, Flash sintering of nanograin zirconia in <5 s at 850°C, J. Am. Ceram. Soc. 93 (2010) 3556–3559.

[14] M. Biesuz, V.M. Sglavo, Flash sintering of ceramics, J. Eur. Ceram. Soc. 39 (2019) 115–143. doi:10.1016/j.jeurceramsoc.2018.08.048.

[15] M. Yu, S. Grasso, R. Mckinnon, T. Saunders, M.J. Reece, Review of flash sintering: materials, mechanisms and modelling, Adv. Appl. Ceram. 116 (2017) 24–60. doi:10.1080/17436753.2016.1251051.

[16] M. Biesuz, V.M. Sglavo, Flash sintering of ceramics, J. Eur. Ceram. Soc. 39 (2019) 115–143. doi:10.1016/j.jeurceramsoc.2018.08.048.

[17] B. Mattan Ze'ev, N. Shomrat, Y. Tsur, Recent Advances in Mechanism Research and Methods for Electric-Field-Assisted Sintering of Ceramics, Adv. Mater. 30 (2018) 1706369. doi:10.1002/adma.201706369.

[18] W. Ji, B. Parker, S. Falco, J.Y. Zhang, Z.Y. Fu, R.I. Todd, Ultra-fast firing: Effect of heating rate on sintering of 3YSZ, with and without an electric field, J. Eur. Ceram. Soc. 37 (2017) 2547–2551.

[19] R. Chaim, Liquid film capillary mechanism for densification of ceramic powders during flash sintering, Materials (Basel). 9 (2016) 19–21. doi:10.3390/ma9040280.

[20] B. Yoon, D. Yadav, R. Raj, E.P. Sortino, S. Ghose, P. Sarin, D. Shoemaker, Measurement of O and Ti atom displacements in TiO2during flash sintering experiments, J. Am. Ceram. Soc. 101 (2018) 1811–1817. doi:10.1111/jace.15375.

[21] M. Biesuz, D. Rizzi, V.M. Sglavo, Electric current effect during the early stages of field-assisted sintering, J. Am. Ceram. Soc. 102 (2019) 813–822. doi:10.1111/jace.15976.

[22] R. Chaim, C. Estournès, Scripta Materialia Effects of the fundamental oxide properties on the

electric fi eld- fl ash temperature during fl ash sintering, Scr. Mater. 163 (2019) 130–132. doi:10.1016/j.scriptamat.2019.01.018.

[23] D. Yadav, R. Raj, The onset of the flash transition in single crystals of cubic zirconia as a function of electric field and temperature, Scr. Mater. 134 (2017) 123–127.

[24] M. Jongmanns, R. Raj, D.E. Wolf, Generation of Frenkel defects above the Debye temperature by proliferation of phonons near the Brillouin zone edge Generation of Frenkel defects above the Debye temperature by proliferation of phonons near the Brillouin zone edge, New J. Phys. 20 (2018) 93013.

[25] D. Kok, S.K. Jha, R. Raj, M.L. Mecartney, Flash sintering of a three-phase alumina, spinel, and yttria-stabilized zirconia composite, J. Am. Ceram. Soc. (2017) 16–19. doi:10.1111/jace.14818.

[26] B. Yoon, D. Yadav, S. Ghose, P. Sarin, R. Raj, E. Program, On the Synchronicity of Flash Sintering and Phase Transformation, 2019. (n.d.) IN PRESS. doi:10.1111/jace.16335.

[27] N. Morisaki, H. Yoshida, K. Matsui, T. Tokunaga, K. Sasaki, T. Yamamoto, Synthesis of zirconium oxynitride in air under DC electric fields, Appl. Phys. Lett. 109 (2016) 83104.

[28] L.M. Jesus, R.S. Silva, R. Raj, J.-C. M'Peko, Electric field-assisted ultrafast synthesis of nanopowders: a novel and cost-efficient approach, RSC Adv. 6 (2016) 107208–107213. doi:10.1039/C6RA18734J.

[29] E. Gil-González, A. Perejón, P.E. Sánchez-Jiménez, M.J. Sayagués, R. Raj, L.A. Pérez-Maqueda, Phase-pure BiFeO3 produced by reaction flash-sintering of Bi2O3 and Fe2O3, Mater. Chem. A. 6 (2018) 5356–5366. doi:10.1039/C7TA09239C.

[30] C. McLaren, W. Heffner, R. Tessarollo, R. Raj, H. Jain, Electric field-induced softening of alkali silicate glasses, Appl. Phys. Lett. 107 (2015) 1–6. doi:10.1063/1.4934945.

[31] L. Pinter, M. Biesuz, V.M. Sglavo, T. Saunders, J. Binner, M. Reece, S. Grasso, DC-electro softening in soda lime silicate glass: An electro-thermal analysis, Scr. Mater. 151 (2018) 14–18. doi:10.1016/j.scriptamat.2018.03.028.

[32] C.T. Mclaren, C. Kopatz, N.J. Smith, H. Jain, Development of highly inhomogeneous temperature profile within electrically heated alkali silicate glasses, Sci. Rep. 9 (2019) 2805. doi:10.1038/s41598-019-39431-8.

[33] H. Yoshida, Y. Sasaki, Low temperature and high strain rate superplastic flow in structural ceramics induced by strong electric-field, Scr. Mater. 146 (2018) 173–177. doi:10.1016/j.scriptamat.2017.11.042.

[34] M. Biesuz, V.M. Sglavo, Current-induced abnormal and oriented grain growth in corundum upon flash sintering, Scr. Mater. 150 (2018) 82–86. doi:10.1016/j.scriptamat.2018.03.004.

[35] P. Tatarko, S. Grasso, T.G. Saunders, V. Casalegno, M. Ferraris, M.J. Reece, Flash joining of CVD-SiC coated C f /SiC composites with a Ti interlayer, J. Eur. Ceram. Soc. 37 (2017) 3841–3848.

[36] X. Zhao, L. Duan, Y. Wang, Fast interdiffusion and Kirkendall effects of SiC-coated C/SiC composites joined by a Ti-Nb-Ti interlayer via spark plasma sintering, J. Eur. Ceram. Soc. (2019) 0–1. doi:10.1016/j.jeurceramsoc.2019.01.020.

[37] J. Xia, K. Ren, Y. Wang, Reversible joining of zirconia to titanium alloy, Ceram. Int. 45 (2018) 2509–2515. doi:10.1016/j.ceramint.2018.10.180.

[38] J. Xia, K. Ren, Y. Wang, L. An, Reversible flash-bonding of zirconia and nickel alloys, Scr. Mater. 153 (2018) 31–34. doi:10.1016/j.scriptamat.2018.04.047.

[39] J. Xia, K. Ren, Y. Wang, Scripta Materialia One-second fl ash joining of zirconia ceramic by an electric fi eld at low temperatures, Scr. Mater. 165 (2019) 34–38. doi:10.1016/j.scriptamat.2019.02.004.

[40] T. Te Chou, W.H. Tuan, H. Nishikawa, B.J. Weng, Brazing Graphite to Aluminum Nitride for Thermal Dissipation Purpose, Adv. Eng. Mater. 19 (2017) 5–10. doi:10.1002/adem.201600876.

[41] L. Xing, J. Lin, M. Huang, W. Yang, Joining of Graphite to Copper with Nb Interlayer: Microstructure and Mechanical Properties, Adv. Eng. Mater. 1800810 (2018) 1–8. doi:10.1002/adem.201800810.

[42] Y. Mao, L. Peng, S. Wang, L. Xi, Microstructural characterization of graphite/CuCrZr joints brazed with CuTiH2Ni-based fillers, J. Alloys Compd. 716 (2017) 81–87. doi:10.1016/j.jallcom.2017.05.019.

[43] R. Dal Maschio, V.M. Sglavo, L. Mattivi, L. Bertamini, S. Sturlese, Indentation Method for Fracture Resistance Determination of Metal/Ceramic Interfaces in Thick TBCs, J. Therm. Spray Technol. 3 (1994) 51–56.

[44] A.G. Evans, M. Ruhle, B.J. Dalgleish, P.G. Charalambides, The Fracture Energy of Bimaterial Interfaces, Metall. Mater. Trans. A. 21A (1990) 2419–2429.

[45] G.D. Sorarù, G. D'Andrea, R. Campostrini, F. Babonneau, G. Mariotto, Structural Characterization and High-Temperature Behavior of Silicon Oxycarbide Glasses Prepared from Sol-Gel Precursors Containing Si-H Bonds, J. Am. Ceram. Soc. 78 (1995) 379–387.

[46] G.T. Burns, R.B. Taylor, A. Zangvil, G.A. Zank, High-Temperature chemistry of the conversion of Siloxanes to Silicon Carbide, Chem. Mater. 4 (1992) 1313–1323.

[47] K.G. Schell, E.C. Bucharsky, R. Oberacker, M.J. Hoffmann, Determination of Subcritical Crack Growth Parameters in Polymer - Derived SiOC Ceramics by Biaxial Bending Tests inWater Environment, J. Am. Ceram. Soc. 93 (2010) 1540–1543. doi:10.1111/j.1551-2916.2009.03566.x.

[48] G.M. Renlund, S. Prochazka, R.H. Doremus, Silicon oxycarbide glasses : Part II . Structure and properties, J. Mater. Res. 6 (1991) 2723–2734.

[49] T. Rouxel, J. Guin, V. Keryvin, G. Soraru, Surface Damage Resistance of Gel-Derived Oxycarbide Glasses: Hardness, Toughness, and Scratchability, J. Am. Ceram. Soc. 84 (2001) 2220–2224.

[50] S.M. Wiedehorn, Fracture Surface Energy of Glass, J. Am. Ceram. Soc. 52 (1969) 99–105.

[51] Kantal super heating elements, (n.d.). https://www.kanthal.com/globalassets/kanthal-global/downloads/furnace-products-and-heating-systems/heating-elements/mosi2-heating-elements/s-ka058-b-eng-2012-01.pdf (accessed March 22, 2019).

[52] J.J. Petrovic, MoSi2-Based Structural Silicides, MRS Bull. (1993) 35–42.

[53] R.U. Vaidya, D.E. Gallegos, D.D. Kautz, Joining of Molybdenum Disilicide to Stainless Steel using Amorphous Metal Brazes-Residual Stress Analysis, in: Conf. Proceeding. DVS-LOT, June 19-21 2007, Aachen, Ger., 2007: p. 7/06.

[54] R.U. Vaidya, A.H. Bartlett, H. Kung, D.P. Butt, Joining of MoSi 2 to itself and reactions with aluminium interlayers, J. Amterials Sci. Lett. 17 (1998) 777–780.

[55] J.F. Xu, X.B. Zhang, Y.J. Fei, H.F. Wu, Y.F. Ye, W. Li, X.B. Zhang, Y.J. Fei, H.F. Wu, Y.F. Ye, W.L. Joining, J.F. Xu, X.B. Zhang, Y.J. Fei, H.F. Wu, Y.F. Ye, W. Li, Joining of MoSi 2 to 316L stainless steel using spark plasma sintering technique, Mater. Sci. Technol. 23 (2007) 875–879. doi:10.1179/174328407X176929.

[56] P. Sebo, P. Svec, M. Zemankova, P. Svec, D. Janickovic, P. Stefanik, Joining of Mo and MoSi2 and their interaction with nickel, Kov. Matrialy. 52 (2014) 324–327. doi:10.4149/km.2014.6.321.

[57] Y. Xu, L. Cheng, L. Zhang, H. Yin, X. Yin, Mechanical properties of 3D fiber reinforced C / SiC composites, Mater. Sci. Eng. A. 300 (2001) 196–202.

[58] W. Krenkel, Carbon Fiber Reinforced CMC for High-Performance Structures, Int. J. Appl. Ceram. Technol. 1 (2004) 188–200.

[59] G.B. Lin, J.H. Huang, H. Zhang, H.Y. Liu, Microstructure and mechanical performance of brazed joints of C f / SiC composite and Ti alloy using Ag – Cu – Ti – W, Sci. Technol. Weld. Join. 11 (2006) 379. doi:10.1179/174329306X113235.

[60] J. Xiong, J. Huang, Z. Wang, G. Lin, H. Zhang, X. Zhao, Joining of C f / SiC composite to Ti alloy using composite filler materials, Mater. Sci. Technol. ISSN. 25 (2009) 1046–1050. doi:10.1179/174328408X378889.

[61] H. Xiong, B. Chen, Y. Pan, H. Zhao, L. Ye, Joining of C f / SiC composite with a Cu – Au – Pd – V brazing filler and interfacial reactions, J. Eur. Ceram. Soc. 34 (2014) 1481–1486. doi:10.1016/j.jeurceramsoc.2013.12.022.

[62] B. Cui, J. Huang, C. Cai, S. Chen, X. Zhao, Microstructures and mechanical properties of C f / SiC composite and TC4 alloy joints brazed with (Ti – Zr – Cu – Ni) + W composite filler materials, Compos. Sci. Technol. 97 (2014) 19–26. doi:10.1016/j.compscitech.2014.03.021.

Flash joining of conductive ceramics in a few seconds by flash spark plasma sintering

Mattia Biesuz [a,b,#], Theo G. Saunders [a], Salvatore Grasso [c], Giorgio Speranza [d], Gian D. Sorarù [b], Renzo Campostrini [b], Vincenzo M. Sglavo [b], Michael J. Reece [a]

[a] Queen Mary University of London, School of Engineering and Materials Science, London E1 4NS, United Kingdom

[b] University of Trento, Department of Industrial Engineering, Via Sommarive 9, 38123, Trento, Italy

[c] Key Laboratory of Advanced technologies of Materials, Ministry of Education, School of Materials Science and Engineering, Southwest Jiaotong University, Chengdu 610031, China

[d] CMM - FBK, Via Sommarive 18, 38123 Trento, Italy

[#] Corresponding author: M.B. mattia.biesuz@outlook.com

Flash joining of graphite: "Ceramization test"

The ceramization of the methyl silicone after FJ (6, 8 and 10 s) was checked using thermal gravimetric analysis coupled with mass spectrometry measurements. The analysis were performed within a home-made system which connect a LabSys Setaram thermobalance with a Trio1 VG quadrupole mass spectrometer. Samples were weighted and loaded into alumina crucible holders (sample weight ~ 10 mg), α-Al_2O_3 was used as reference. The treatments were carried out in He atmosphere (He flow = 120 cm^3/min) using an heating rate of 10°C/min. During the thermal analysis an appropriate fraction of the purging He flux, was continuously withdrawn and analyzed by the mass detector by using a silica deactivate capillary column (0.32 mm internal diameter, 13.5 m length, 140°C).

The measured weight loss during the test was in the order of 0.1-0.2 mg (1-2 wt%, Figure S1), which falls within the accuracy of the measurement (due to the buoyancy effect). Moreover, no mass spectrometry (MS) signals associated to CO_2, CO, CH_4, SiH_4, methyl silane were detected, thus pointing out a complete ceramization of the material during FJ.

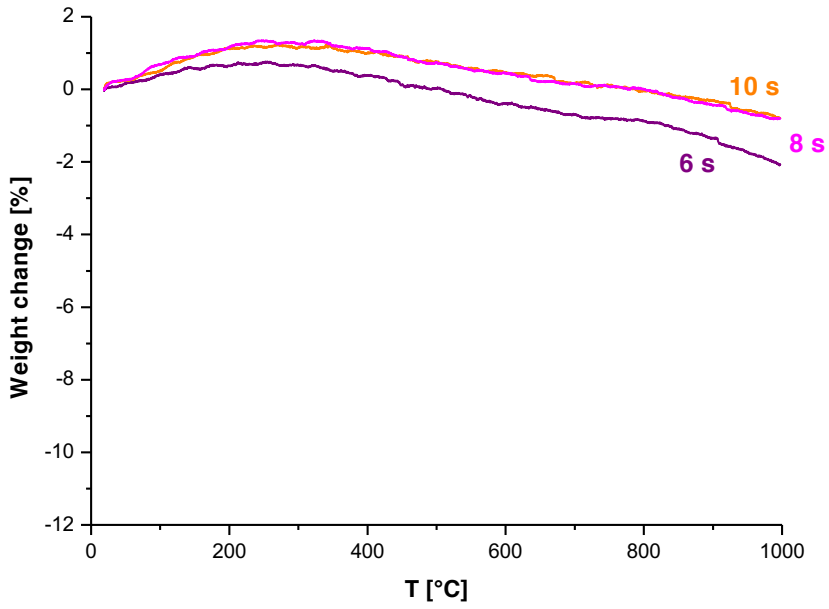

Figure S1: TG analysis carried out on samples pyrolyzed in flash-SPS configuration for 6, 8 and 10 s.

Flash joining of C_f-SiC composite

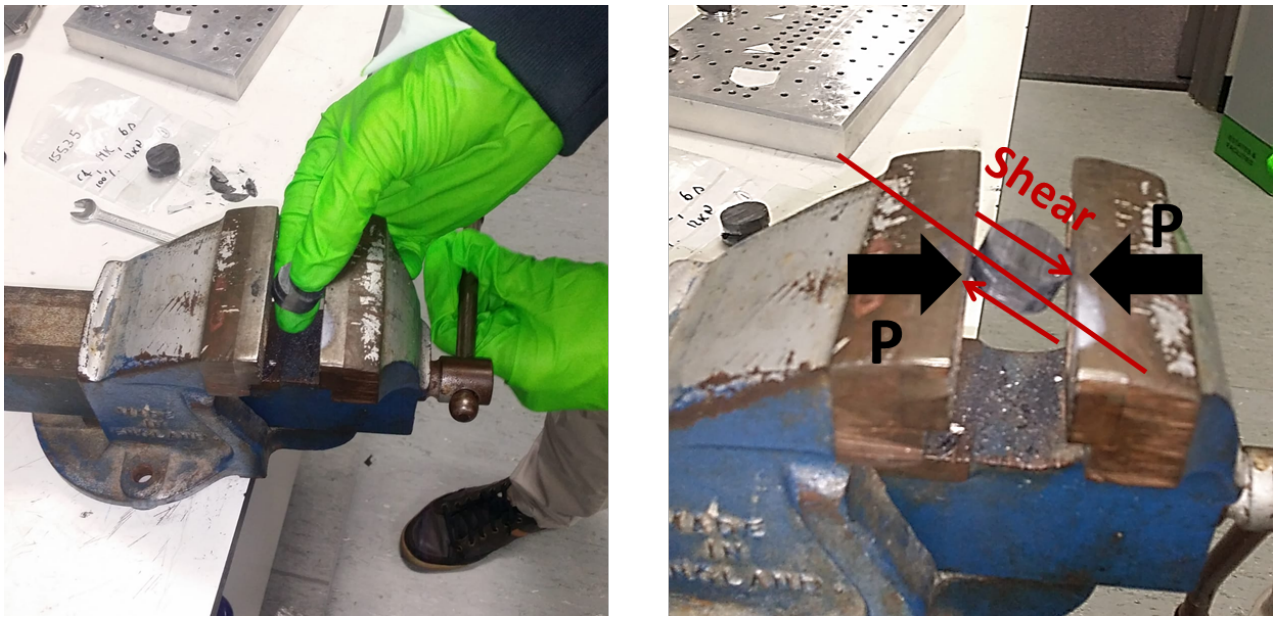

Figure S2: Vise-sample configuration used to produce delamination of the C_f-SiC composite after flash joining.

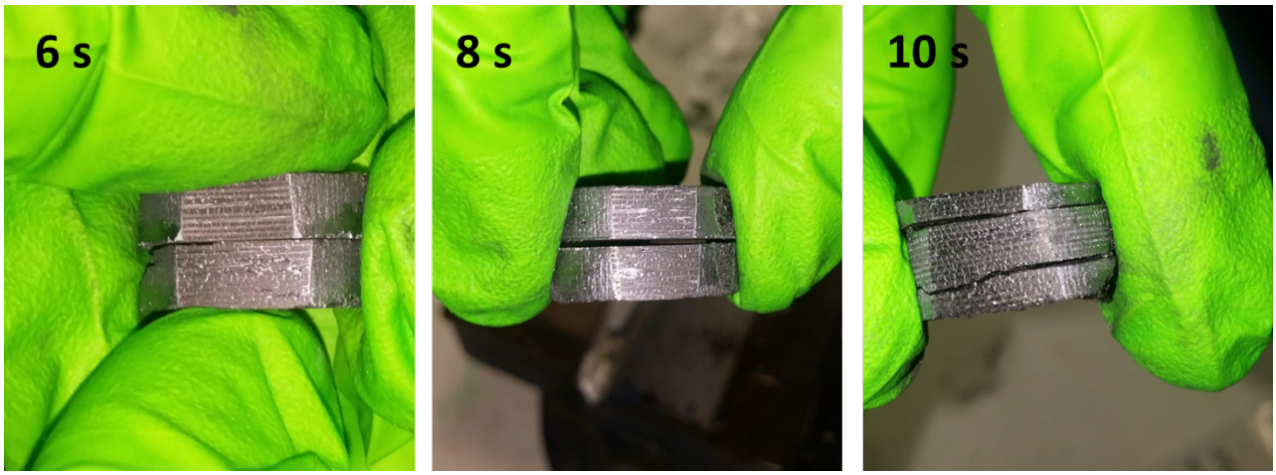

Figure S3: Flash joined C_f-SiC composite after delamination (Figure S1).

Acknowledgements

The authors gratefully acknowledge the JECS Trust for funding the visit of M. Biesuz to the Queen Mary University of London (Contract No. 2018172).

This material is based upon work supported by the Air Force Office of Scientific Research under award number FA9550-17-1-0526.